Expression of chemokine receptor CXCR3 on T cells affects the balance between effector and memory CD8 T-cell generation

Joyce K. Hu[a,b], Takashi Kagari[a,1], Jonathan M. Clingan[a,b], and Mehrdad Matloubian[a,2]

[a]Division of Rheumatology, Department of Medicine, and Rosalind Russell Medical Research Center for Arthritis, and [b]Graduate Program in Biomedical Sciences, University of California, San Francisco, CA 94143

Edited* by Arthur Weiss, University of California, San Francisco, CA, and approved April 6, 2011 (received for review February 2, 2011)

Generation of a robust immunological memory response is essential for protection on subsequent encounters with the same pathogen. The magnitude and quality of the memory CD8 T-cell population are shaped and influenced by the strength and duration of the initial antigenic stimulus as well as by inflammatory cytokines. Although chemokine receptors have been established to play a role in recruitment of effector CD8 T cells to sites of inflammation, their contribution to determination of T-cell fate and shaping of the long-lived memory T-cell population is not fully understood. Here, we investigated whether reduced access to antigen and inflammation through alterations in expression of inflammatory and homeostatic chemokine receptors has an impact on generation of effector and memory CD8 T cells. We found that in mice infected with lymphocytic choriomeningitis virus, colocalization of virus-specific CD8 T cells with antigen in spleen is dependent on expression of the inflammatory chemokine receptor, CXCR3. In addition, absence of CXCR3 expression on CD8 T cells leads to formation of fewer short-lived effector cells and more memory precursor cells. Furthermore, the memory CD8 T-cell population derived from CXCR3-deficient cells has fewer cells of the effector memory phenotype and exhibits a recall response of greater magnitude than that of WT cells. These data demonstrate that CD8 T-cell positioning relative to antigen and inflammatory cytokines in secondary lymphoid organs affects the balance of effector and memory T-cell formation and has both a quantitative and qualitative impact on the long-lived memory CD8 T-cell population.

microenvironment | T-cell differentiation | trafficking

In response to an infection with an intracellular pathogen, antigen-specific CD8 T cells undergo rapid clonal expansion while differentiating into cytotoxic effector T cells that then control the infection through lysis of the infected cells and production of cytokines (1). After the peak of the expansion, the majority of effector T cells undergo apoptosis, leaving behind a small fraction that give rise to long-lived, self-renewing memory CD8 T cells with a superior recall response to the same antigen. In the past decade, major advances have been made in our understanding of the lineage relationship between short-lived effector cells and the precursor cells that give rise to long-lived memory CD8 T cells. Elegant cell tracing studies have shown that an individual naive CD8 T cell can have multiple fates and give rise to both short-lived effector and long-lived memory cells (2). The proportion of effector cells that gives rise to long-lived memory cells can be affected by several factors, including the strength and duration of antigenic stimulus as well as proinflammatory cytokines and other environmental factors. Progress in identification of terminal effector and memory precursor cells within the heterogeneous effector population at early times after infection, through their expression of such markers as KLRG-1 and IL-7Rα, has paved the way for elucidating how cell intrinsic and extrinsic factors, including positional cues, alter the balance between effector and memory T-cell generation (3, 4).

Naive CD8 T cells continuously circulate between blood and secondary lymphoid organs in search of their cognate antigen. They express high levels of CCR7, and thus localize within the T-zone areas of the spleen and lymph nodes, where the CCR7 ligands CCL19 and CCL21 are homeostatically expressed. On activation by both antigen and innate stimuli, such as type I interferons, CD8 T cells alter their expression of chemokine receptors (5). Receptors, such as CCR7 and S1PR1, are down-regulated, and inflammatory chemokine receptors, such as CXCR3, CXCR6, and CCR5, are up-regulated (6–9). These receptors then guide effector CD8 T cells toward activated dendritic cells to receive further "help" from CD4 T cells or recruit them to inflamed tissues to control the infection. One particular receptor, CXCR3, has been shown to be important in recruitment of effector CD8 T cells to allografts and sites of viral infection within the CNS and genital tract, where its ligands, CXCL9 and CXCL10, are induced by IFN-γ (10–15).

In addition to regulating the trafficking patterns of effector CD8 T cells, chemokine receptors have an impact on the interaction of these cells with their microenvironment. How chemokine receptors influence these interactions and affect CD8 T-cell differentiation is not completely understood. In this study, we examined the role of CXCR3 in differentiation of activated CD8 T cells in vivo in response to infection of the host with lymphocytic choriomeningitis virus (LCMV). We found that absence of CXCR3 on CD8 T cells leads to less colocalization of effector T cells with antigen within the spleen and affects the balance between generation of short-lived effector and memory precursor cells. More strikingly, absence of CXCR3 leads to generation of more long-lived memory CD8 T cells with a qualitatively better recall response.

Results

CXCR3 Is Gradually Up-Regulated on Antigen-Specific CD8 T Cells During the Course of Infection. To determine whether chemokine receptors play a role in CD8 T-cell fate determination after activation, we analyzed expression of a number of these receptors on Ag-specific CD8 T cells following LCMV infection. One particular receptor, CXCR3, was up-regulated approximately 10-fold as early as day 3 postinfection on P14 T-cell receptor (TCR) transgenic (Tg) CD8 T cells specific for LCMV D^bGP33-41 (Fig. 1*A*).

Author contributions: J.K.H., T.K., and M.M. designed research; J.K.H., T.K., J.M.C., and M.M. performed research; J.K.H. and J.M.C. analyzed data; and J.K.H. and M.M. wrote the paper.

The authors declare no conflict of interest.

*This Direct Submission article had a prearranged editor.

[1]Present address: Frontier Research Laboratories, Daiichi Sankyo Co., Ltd., Tokyo 134-8630, Japan.

[2]To whom correspondence should be addressed. E-mail: mehrdad.matloubian@ucsf.edu.

See Author Summary on page 8535.

This article contains supporting information online at www.pnas.org/lookup/suppl/doi:10.1073/pnas.1101881108/-/DCSupplemental.

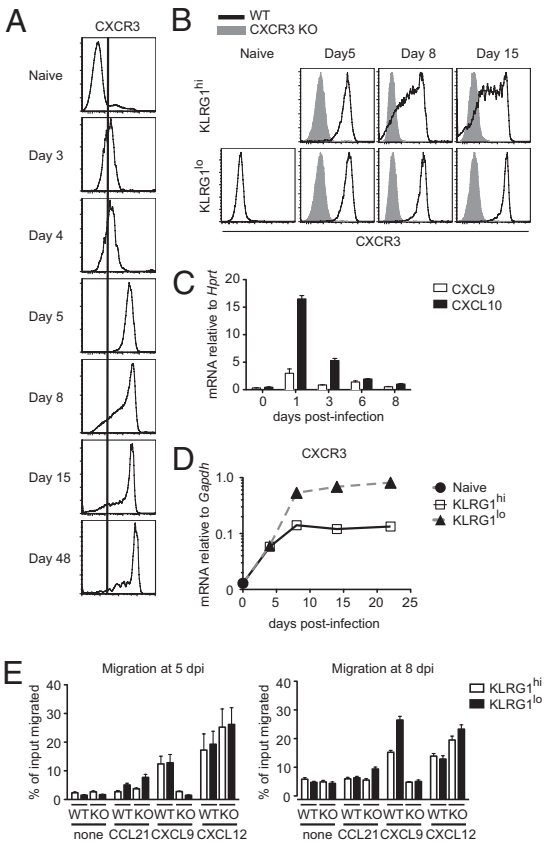

Fig. 1. CXCR3 is gradually up-regulated on antigen-specific CD8 T cells during the course of infection. C57BL/6 mice containing CD45.1/CD45.2 WT P14 T cells were infected with LCMV. (*A*) Expression of CXCR3 on splenic P14 T cells was determined by flow cytometry at the indicated times after infection. Plots are gated on $CD8^+$ $CD45.1^+$ P14 T cells. (*B*) Cell surface expression of CXCR3 on $KLRG1^{hi}$ and $KLRG1^{lo}$ subsets of P14 T cells was determined at the indicated times after infection. Data shown in *A* and *B* are representative of three independent experiments ($n = 6$ for each time). (*C*) Expression of mRNA for CXCR3 ligands CXCL9 and CXCL10 in spleen samples was measured by quantitative RT-PCR at the indicated times after infection. Data from one representative experiment are shown ($n = 2$–3 for each time). (*D*) Expression of CXCR3 mRNA in sorted $KLRG1^{hi}$ and $KLRG1^{lo}$ P14 T cells was measured by quantitative RT-PCR at the indicated times. Data shown are averages of three independently sorted samples. The graphs in *C* and *D* show mean data ± SEM. (*E*) Chemotactic response of splenic $KLRG1^{hi}$ and $KLRG1^{lo}$ WT and CXCR3-deficient P14 T cells to 1 $\mu g \cdot mL^{-1}$ CCL21, 1 $\mu g \cdot mL^{-1}$ CXCL9, and 0.3 $\mu g \cdot mL^{-1}$ CXCL12 was determined at the indicated times after infection. Data shown are averages of duplicate samples, with bars representing the range.

CXCR3 expression reached peak levels by day 5 postinfection but was then partially down-regulated on a small fraction of the cells by day 8 postinfection (Fig. 1*A*). Several recent studies have shown that within the heterogeneous effector CD8 T-cell population, level of expression of KLRG1 can distinguish those cells that are terminally differentiated and are destined to die ($KLRG1^{hi}$) from those that give rise to long-lived memory cells ($KLRG1^{lo}$) (3, 4). Further analysis of $KLRG1^{hi}$ and $KLRG1^{lo}$ subsets of effector CD8 T cells showed that both populations expressed similar levels of CXCR3 at day 5 postinfection (Fig. 1*B*). The $KLRG1^{hi}$ terminally differentiated CD8 T cells had reduced levels of CXCR3 expression by day 8, however, whereas the $KLRG1^{lo}$ memory precursor cells maintained uniform and stable high levels of CXCR3 expression (Fig. 1*B*). Of the three known CXCR3 ligands, C57BL/6 mice express only two, CXCL9 and CXCL10 (16–19). As determined by quantitative RT-PCR, both ligands were up-regulated in spleens of mice on day 1 postinfection and were maintained at somewhat lower levels throughout the course of infection (Fig. 1*C*). The continuous presence of CXCR3 ligands in the spleen suggested that lower expression of CXCR3 on $KLRG1^{hi}$ cells may be attributable to ligand-induced receptor endocytosis, because this population may be localized differently within the spleen than the $KLRG1^{lo}$ subset and may encounter different amounts of CXCR3 ligands (20). To address this possibility, we evaluated CXCR3 mRNA expression by quantitative RT-PCR in sorted $KLRG1^{hi}$ and $KLRG1^{lo}$ CD8 effector populations at various times after in vivo activation. Consistent with cell surface CXCR3 expression, both populations had similar levels of CXCR3 mRNA at day 4 postinfection (Fig. 1*D*). By day 8, however, the $KLRG1^{lo}$ subset had approximately 5-fold higher CXCR3 mRNA expression than the $KLRG1^{hi}$ T cells. Similarly, in a functional chemotaxis assay, we did not find any differences in migration of $KLRG1^{hi}$ and $KLRG1^{lo}$ CD8 T cells to CXCL9 on day 5 postinfection (Fig. 1*E*). Consistent with CXCR3 expression data, however, by day 8 postinfection, $KLRG1^{hi}$ cells had a somewhat lower chemotactic response to CXCL9 compared with $KLRG1^{lo}$ cells (Fig. 1*E*).

Absence of CXCR3 Expression on CD8 T Cells Leads to the Development of More Memory Precursor and Fewer Terminally Differentiated Effector CD8 T Cells. CXCR3 and its ligands have been implicated as playing a role in the trafficking of effector CD8 T cells to specific organs in several microbial infections and allograft rejection (10, 11, 14, 15, 21–24). To determine whether CXCR3 also influences the generation of effector and memory CD8 T cells, we cotransferred WT and CXCR3-deficient P14 T cells expressing different CD45 congenic alleles into WT mice and followed their expansion and phenotype in response to infection with LCMV. In spleen, at the peak of the CD8 T-cell response, we consistently found a slightly higher proportion of WT P14 cells compared with those lacking CXCR3 (Fig. 2*A*). This was not attributable to a global alteration in CD8 T-cell trafficking, because similar differences were observed in blood (Fig. 2*A*). More strikingly, compared with WT cells, a smaller proportion of CXCR3-deficient cells had phenotypic characteristics of short-lived effector cells ($KLRG\text{-}1^{hi}$ $IL\text{-}7R\alpha^{lo}$) and a greater proportion expressed markers of memory precursor effector cells ($KLRG\text{-}1^{lo}$ $IL\text{-}7R\alpha^{hi}$) (Fig. 2*A*). This shift in effector population subsets became evident at the peak of the response on day 8 and corresponded to a modest decrease in the number of CXCR3-deficient short-lived effector cells. In contrast, the number of CXCR3-deficient memory precursor cells was increased (Fig. 2 *A* and *C*). We did not observe any differences between WT and CXCR3-deficient cells at the peak of the response with respect to expression of several activation markers and the ability to make the effector cytokines IFN-γ and TNF-α (Fig. 2*B*). These data suggest that expression of CXCR3 favors the development of short-lived effector CD8 T cells as opposed to memory precursor cells.

Restoration of CXCR3 Expression in CXCR3-Deficient CD8 T Cells Leads to Development of More Terminally Differentiated Effector Cells and Fewer Memory Precursor Cells. To determine further whether expression of CXCR3 can drive differentiation of activated CD8 T cells toward short-lived effector cells rather than long-term memory cells, we used a mouse stem cell virus (MSCV)-based retroviral vector to express mouse CXCR3 in CXCR3-deficient P14 cells. CXCR3-deficient T cells were activated in vivo and then transduced ex vivo with a construct containing mouse CXCR3 followed by IRES-Thy1.1, which allows one to distinguish between transduced and nontransduced cells within the same starting population (Fig. 3*A*). Shortly after transduction, the cells were transferred into mice that were infected several hours earlier with LCMV, and the fate of the cells was then followed in vivo. Expression of CXCR3 on transduced cells was

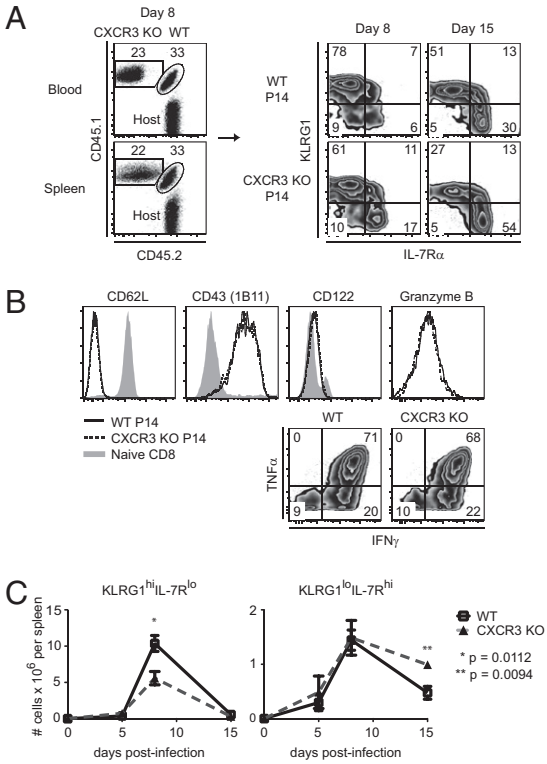

Fig. 2. Absence of CXCR3 expression on CD8 T cells leads to the development of more memory precursor and fewer terminally differentiated effector CD8 T cells. Mice containing equal numbers of CD45.1/CD45.2 WT and CD45.1/CD45.1 CXCR3 KO P14 T cells were infected with LCMV. (*A*) (*Left*) Dot plots show frequencies of WT and CXCR3 KO P14 T cells within the CD8 T-cell population in blood and spleen on day 8 postinfection. (*Right*) Density plots show surface expression of KLRG1 and IL-7Rα on WT and CXCR3 KO P14 T cells in spleen at the indicated times after infection. (*B*) Expression levels of cell surface markers and intracellular cytokines in WT and CXCR3 KO P14 T cells were determined on day 8 postinfection. (*C*) Total numbers of KLRG1^{hi}IL-7R^{lo} and KLRG1^{lo}IL-7R^{hi} subsets of WT and CXCR3 KO P14 T cells in spleen were determined at the indicated times after infection. (*A–C*) Data are representative of three independent experiments (n = 4–8 for each time). The graphs show mean data ± SEM. Statistics were done using a two-tailed unpaired Student's t test.

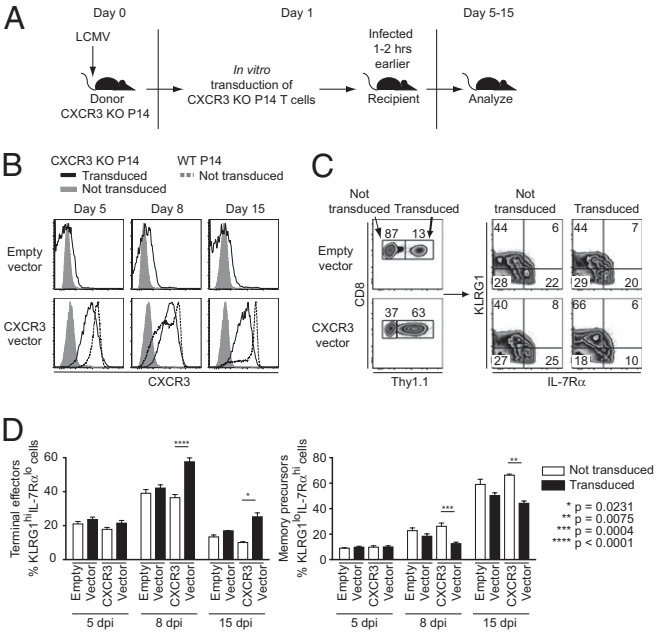

Fig. 3. Restoration of CXCR3 expression in CXCR3-deficient CD8 T cells leads to development of more terminally differentiated effector and fewer memory precursor cells. (*A*) CD45.1$^+$ CXCR3-deficient P14 T cells were activated in vivo; the next day, they were transduced ex vivo with retroviral preparations expressing either nothing (empty vector) or mouse CXCR3 followed by IRES-Thy1.1. C57BL/6 mice that were infected a few hours earlier with LCMV received 2 × 10^5 transduced CXCR3 KO P14 T cells and were analyzed at the indicated times after infection. (*B*) Surface expression of CXCR3 on transduced CXCR3 KO P14 T cells in spleens of recipients was determined at the indicated times after infection. Histograms are gated on CD8$^+$ CD45.1$^+$ Thy1.1$^+$ transduced or CD8$^+$ CD45.1$^+$ Thy1.1$^-$ nontransduced CXCR3 KO P14 T cells within the same recipient mouse. Dotted histograms show CXCR3 expression on WT P14 T cells at the indicated times. (*C*) Transduced (Thy1.1$^+$) and nontransduced (Thy1.1$^-$) cells were gated from adoptively transferred CXCR3 KO P14 T cells and analyzed for surface expression of KLRG1 and IL-7Rα. (*D*) Frequencies of KLRG1^{hi}IL-7R^{lo} and KLRG1^{lo}IL-7R^{hi} effector cell subsets in transduced (black bars) and nontransduced (white bars) CXCR3 KO P14 T cells in spleens of recipient mice were determined at the indicated times after infection. dpi, days postinfection. Data shown in *A–D* are representative of three independent experiments (n = 2–8 per group per day). The graphs show mean ± SEM. Statistics were done using a two-tailed unpaired Student's t test.

slightly lower than on WT nontransduced P14 cells (Fig. 3*B*). Restoration of partial CXCR3 expression led to greater expansion of P14 T cells in vivo and the generation of more short-lived effector cells (KLRG-1^{hi} IL-7Rα^{lo}) at the expense of long-lived memory precursor cells (KLRG-1^{lo} IL-7Rα^{hi}) (Fig. 3*C*). Similar to what was observed when we compared WT and CXCR3-deficient P14 cells (Fig. 2*C*), the effect of CXCR3 expression on CD8 effector T-cell differentiation was evident only at the peak of the response and during the contraction phase but not at day 5 postinfection (Fig. 3*D*). These data suggest that although CXCR3 is not a major determinant of CD8 T-cell activation and proliferation, its expression can affect the later stages of the CD8 response and have a negative impact on the generation of long-lived memory T cells.

In addition to affecting CD8 T-cell fate, retroviral-mediated expression of CXCR3 affected expansion of effector CD8 T cells. At the peak of the response, we found a greater proportion of CXCR3-transduced cells to be Thy1.1$^+$ compared with those transduced with the control empty vector, despite similar initial transduction efficiencies (Fig. 3*C*). Because CXCR3 is expressed only on a small subset of naive P14 T cells (Fig. 1*A*), these results suggested that early retroviral expression of CXCR3 might facilitate exposure of CD8 T cells to antigen and further drive their expansion. We relied on the observation that about 10–15% of naive P14 T cells express CXCR3 to test this hypothesis by cotransferring either sorted CXCR3$^+$ or CXCR3$^-$ WT P14 cells with CXCR3 KO cells and determining their expansion and differentiation (Fig. S1*A*). When CXCR3$^+$ WT P14 cells were cotransferred with CXCR3 KO cells, WT cells expanded four- to fivefold more in number. In contrast, when WT P14 cells that lacked CXCR3 expression were used, the WT cells expanded only two- to threefold more than CXCR3 KO cells (Fig. S1*B*). Regardless of whether the starting WT population expressed CXCR3 or not at the time of transfer, within the effector population at the peak of the response, there were proportionately more terminally differentiated effector cells (KLRG-1^{hi} IL-7Rα^{lo}) and fewer memory precursor cells (KLRG-1^{lo} IL-7Rα^{hi}) than in the CXCR3 KO population (Fig. S1*B*). These results suggest that the differences observed between WT and CXCR3-deficient P14 T cells are not attributable to expression of CXCR3 on a subpopulation of naive WT cells during the initial stages of activation.

Absence of CXCR3 Leads to More Rapid Phenotypic and Functional Maturation of Memory CD8 T Cells. To examine further the impact of CXCR3 expression on CD8 T-cell memory development, we

analyzed the phenotype and distribution of WT and CXCR3-deficient P14 TCR Tg T cells in various tissues within the same animal after day 40 and up to day 356 postimmunization. We consistently found approximately two- to fourfold more CXCR3-deficient memory CD8 T cells than WT cells within the same recipient in all the examined tissues (Fig. 4*A*). At earlier times after immunization, compared with WT, a greater proportion of CXCR3-deficient P14 memory cells were KLRG1^{lo} IL-7Rα^{hi}, consistent with a faster transition to a more mature memory population (25) (Fig. 4*B*). Similarly, compared with WT memory cells, a smaller proportion of CXCR3-deficient cells had phenotypic characteristics of effector memory cells (CCR7^{lo} CD62L^{lo}) (26) (Fig. 4*B*). These differences were observed in all the examined tissues, ruling out a contribution from differential trafficking patterns, and gradually diminished over time, suggesting that the CXCR3-deficient cells had acquired a more mature memory

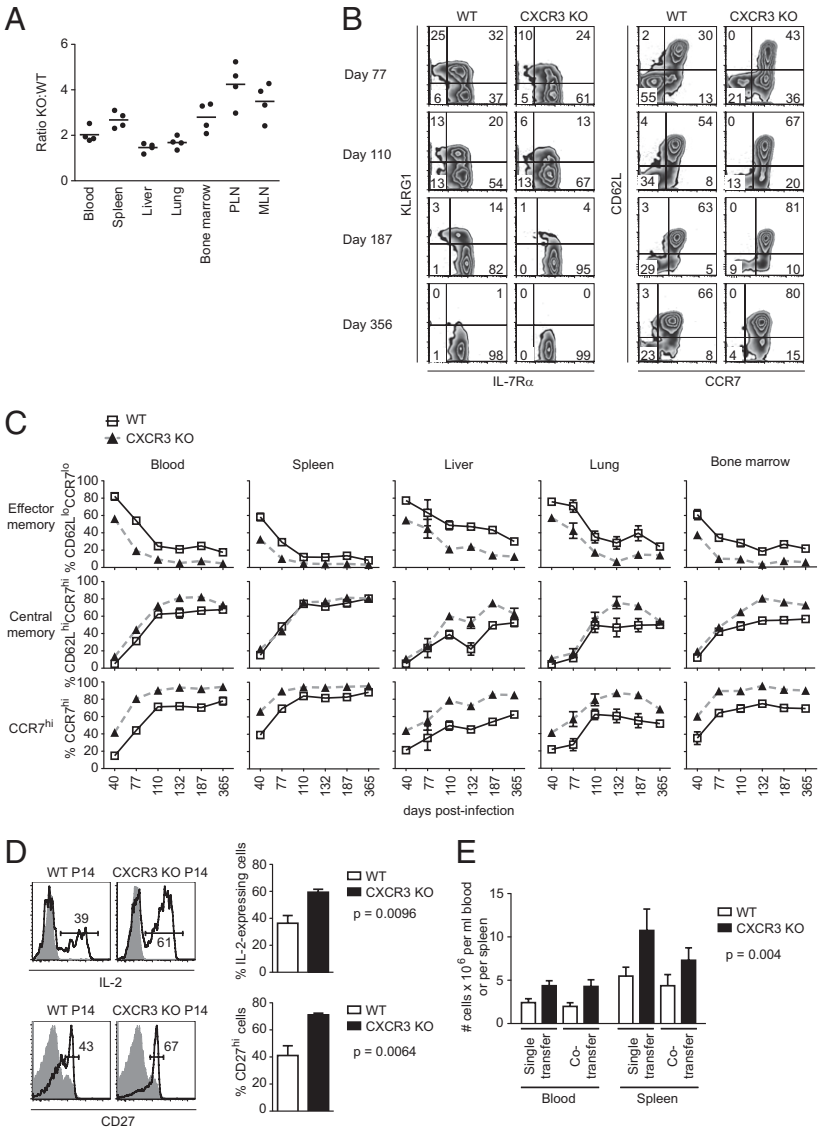

Fig. 4. Absence of CXCR3 leads to more rapid phenotypic and functional maturation of memory CD8 T cells. (*A–C*) C57BL/6 mice containing equal numbers of WT and CXCR3 KO P14 T cells were infected with LCMV. (*A*) Ratio of CXCR3 KO to WT memory P14 T cells in blood or in the indicated tissues. Data are combined for days 40 and 60 postinfection ($n = 2$ mice for each time) and are representative of three experiments. MLN, mesenteric lymph nodes; PLN, peripheral lymph nodes. (*B*) At the indicated times after infection, WT and CXCR3 KO memory P14 T cells in blood were analyzed by flow cytometry for expression of KLRG1 and IL-7Rα (*Left*) and CD62L and CCR7 (*Right*). Plots show data from one representative experiment ($n = 2–4$ mice for each time). (*C*) Frequencies of effector memory (CD62L^{lo} CCR7^{lo}), central memory (CD62L^{hi} CCR7^{hi}), and CCR7^{hi} cells in WT and CXCR3 KO P14 T-cell populations in various tissues were determined at the indicated times after infection. Plots show combined data from three independent experiments ($n = 2–4$ for each time). (*D*) Histograms show the proportion of WT and CXCR3 KO memory P14 T cells in the spleen that express IL-2 or CD27 on days 60 and 40 postinfection, respectively. Gray histograms correspond to unstimulated P14 T cells for IL-2 and non-TCR Tg naive CD8 T cells for CD27. The corresponding bar graphs show the frequencies of IL-2–expressing cells and CD27^{hi} cells in the spleen. Data are from two independent experiments ($n = 4$ mice per group). Statistics were done using a two-tailed unpaired Student's *t* test. (*E*) Recall response of WT and CXCR3 KO memory P14 T cells to secondary infection. B6.BoyJ (CD45.1) mice containing CD45.2/CD45.2 WT P14 T cells and C57BL/6 mice containing CD45.1/CD45.1 CXCR3 KO P14 T cells were infected with LCMV. After 110 d postinfection, memory cells were sorted and 5×10^3 CD62L$^+$ WT and 5×10^3 CD62L$^+$ CXCR3 KO memory P14 T cells were transferred either separately (single transfer) or together in a 1:1 ratio (cotransfer) into naive mice. Two days later, recipients were infected i.v. with 2×10^6 PFU LCMV, and the number of WT and CXCR3 KO P14 T cells in blood and spleen was determined at day 8 postinfection. Data shown are representative of three experiments ($n = 7$ mice per group). The graphs show mean data ± SEM. Statistics were performed using two-way ANOVA.

phenotype more rapidly than WT cells (27) (Fig. 4*C*). Alternatively, CXCR3-deficient memory precursor cells might be less likely to give rise to effector memory cells. The greatest difference we observed between WT and CXCR3-deficient memory CD8 T cells was within the $CD62L^{lo}$ population. In the absence of CXCR3, a greater proportion of this population was $CCR7^{hi}$ at all the examined times after infection. This $CD62L^{lo}$ $CCR7^{hi}$ population may represent a transitional state to the central memory phenotype because these cells express very high and uniform levels of CXCR3, similar to the $KLRG1^{lo}$ $IL\text{-}7R\alpha^{hi}$ and central memory ($CD62L^{hi}$ $CCR7^{hi}$) populations (Fig. S2). In contrast, effector memory cells, postulated to descend mostly from the $KLRG1^{hi}$ population, express lower levels of CXCR3, consistent with expression on the $KLRG1^{hi}$ population (4) (Fig. S2).

In addition to cell surface phenotypic differences and consistent with a more mature functional memory phenotype, a greater proportion of CXCR3-deficient memory CD8 T cells were capable of producing IL-2 and were $CD27^{hi}$ compared with WT cells (Fig. 4*D*). To determine whether there were any additional functional differences between WT and CXCR3-deficient memory CD8 T cells, $CD62L^{hi}$ P14 memory cells of each genotype were sorted and transferred either separately or together at a 1:1 ratio into groups of naive mice. Recipient mice were challenged with LCMV, and at the peak of the secondary response, we found that regardless of whether the two populations were transferred together or separately, there were about twofold more CXCR3-deficient CD8 T cells compared with WT cells (Fig. 4*E*). Similar differences were observed in the secondary response of sorted $CD62L^{lo}$ memory populations, although consistent with other reports, the extent of proliferation was much lower than that of $CD62L^{hi}$ memory cells (27). These results indicate that the CXCR3-deficient memory CD8 T cells have a higher proliferative response, and are thus functionally more mature than WT cells.

A major advantage of using a TCR Tg system is that the contribution of a specific molecule to T-cell function can be evaluated by comparing cells that are sufficient and deficient for that molecule within the same organism. To determine whether our observations were restricted to a TCR Tg system or were more widely applicable to CD8 T-cell biology, we generated mixed bone marrow chimeras by reconstituting lethally irradiated mice with a 1:1 mixture of WT and CXCR3-deficient bone marrow cells with CD45 congenic haplotypes distinct from each other and the recipient mice. As a control, a group of mice was reconstituted with a 1:1 mixture of WT bone marrow cells of differing CD45 congenic haplotypes as well. The ratio of CXCR3-deficient and CXCR3-sufficient CD8 T cells was determined before immunization with LCMV. At the peak of the effector response and during the memory phase, the frequency of CD8 T cells specific for the major epitopes of LCMV in each population was determined by tetramer staining. Similar to the results obtained with the Tg system, there were fewer CXCR3-deficient effector cells compared with WT cells at the peak of the response and relatively more CXCR3-deficient memory cells in the later stages (Fig. S3 *A* and *C*). Consistent differences were not observed between CD8 T cells derived from either WT donor bone marrow cells in control chimeras (Fig. S3 *B* and *D*). These results suggest that the effect of CXCR3 on generation of effector and memory CD8 T cells is not restricted to the TCR Tg system.

Effector CD8 T Cells Colocalize in the Spleen with Antigen and CXCL9 in a CXCR3-Dependent Manner. The role of CXCR3 in trafficking of effector CD8 T cells to inflamed organs, and especially the CNS, has been well established. Very little is known about the function of CXCR3 in localization of responding CD8 T cells within a lymphoid organ during the course of an immune response, however. We hypothesized that such differences in localization may contribute to effector CD8 T-cell fate determination. To address this question, WT and CXCR3-deficient naive P14 cells expressing distinct congenic alleles of CD45 and Thy1 were cotransferred in a 1:1 ratio into naive mice. At different times after infection with LCMV, localization of the responding cells, as well as viral antigen and CXCL9 (a CXCR3 ligand), was determined by immunofluorescent staining of spleen sections. Consistent with previous reports, we found the majority of LCMV antigen localized within the marginal zone of the spleen and diminished in amount by day 5 postinfection (28) (Fig. 5*A*). In addition, CXCL9 was localized in the same area as viral antigen, and marginal zone macrophages sorted from LCMV-infected mice contained high levels of both viral RNA and mRNA for the CXCR3 ligands, CXCL9 and CXCL10 (Fig. 5 *A* and *B*). Even though viral antigen was less readily visualized by day 5 postinfection, CXCL9 could still be detected in sections. Within the same spleen, WT P14 T cells colocalized with CXCL9 and viral antigen in the marginal zone area, whereas CXCR3-deficient P14 T cells were mostly found within the T-zone area and were less readily found associated with CXCL9 and viral antigen (Fig. 5 *A* and *C* and Fig. S4). These results show that CXCR3 can affect localization of effector CD8 T cells within secondary lymphoid organs and provide more or prolonged access to antigen.

CXCR3-Deficient CD8 T Cells Show Reduced Proliferation During the Later Stages of Infection. We have found that activated CXCR3-deficient CD8 T cells do not colocalize as effectively as WT cells with antigen in vivo and produce fewer terminally differentiated effector cells and more central memory cells. To delineate more specifically the stage at which CXCR3 affects CD8 T-cell responses, we examined activation, proliferation, and survival of WT and CXCR3-deficient P14 T cells in vivo at various times after infection. CXCR3 expression was not required for early events of activation and proliferation, because there were no differences between WT and KO cells in up-regulation of CD25 on day 1 postinfection and in 5-(and-6)-carboxyfluorescein diacetate succinimidyl ester (CFSE) dilution by day 2.5 postinfection (Fig. 6 *A* and *B*). These results were not entirely unexpected, because CXCR3 was not highly expressed on CD8 T cells during early stages of activation (Fig. 1 *A* and *D*). Because the earliest effects of CXCR3 were observed between days 5 and 8 postinfection, we examined the survival and proliferation of activated CD8 T cells during this period. We did not observe any differences in the frequency of dying WT and KO cells, as measured by annexin V staining (Fig. 6C). Similarly, there was no effect of CXCR3 expression on the proportion of CD8 T cells that incorporated BrdU on day 5 postinfection. On days 6 and 7 postinfection, however, approximately half as many CXCR3-deficient CD8 T cells incorporated BrdU relative to WT cells (Fig. 6*D*). Further phenotypic characterization of CD8 T cells based on expression of KLRG1 and IL-7Rα showed that the greatest difference between WT and KO cells in BrdU incorporation was in the $KLRG1^{lo}$ $IL\text{-}7R\alpha^{lo}$ population (Fig. 6*E*). This population has been shown to give rise mostly to long-lived memory CD8 T cells but also to retain the potential to become terminally differentiated effector cells (3, 4). Because the $KLRG1^{lo}$ $IL\text{-}7R\alpha^{lo}$ CD8 T cells also express CXCR3, our data suggest that further exposure to antigen and inflammatory stimuli driven by this chemokine receptor may affect the balance between generation of terminally differentiated effector cells and long-lived memory cells as well as the quality of the latter population. The effect of CXCR3 on the production of terminal effectors and memory precursors occurs toward the end of the CD8 T-cell response and is consistent with the fate commitment with progressive differentiation model (29, 30).

Persistent CCR7 Expression Tips the Balance Toward the Development of More Memory Precursors Than Terminally Differentiated Effector CD8 T Cells. Our results suggest that inflammatory chemokine receptors, such as CXCR3, can affect differentiation of activated

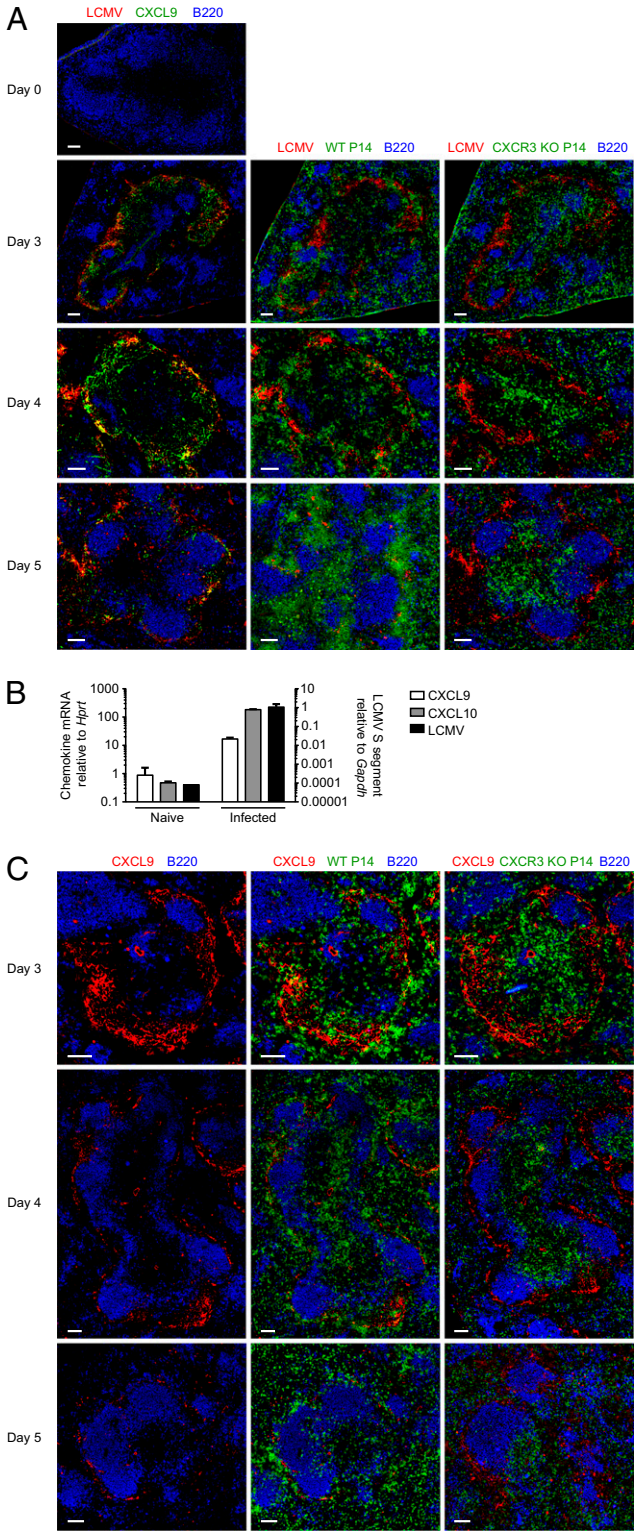

Fig. 5. Effector CD8 T cells colocalize in the spleen with antigen and CXCL9 in a CXCR3-dependent manner. (*A* and *C*) Equal numbers of Thy1.1$^+$ WT and CD45.1/CD45.1 CXCR3 KO P14 T cells were cotransferred into C57BL/6 recipients that were then infected with LCMV. Consecutive sections were prepared from spleens taken at the indicated times after infection and were stained for viral antigen, CXCL9, WT P14 (Thy1.1), CXCR3 KO P14 (CD45.1), and B220. Data are representative of two independent experiments (n = 4 for each time). (Scale bar: 100 μm.) (*B*) Expression of LCMV RNA or mRNA for CXCR3 ligands, CXCL9 and CXCL10, in marginal zone macrophages sorted from naive mice or those infected a day earlier with LCMV was determined by quantitative RT-PCR. Expression is shown relative to *Gapdh* for LCMV RNA and relative to *Hprt* for CXCL9 and CXCL10. Data shown are averages of two independent sorted samples (n = 4–5 mice for each sample).

CD8 T cells by promoting encounters with antigen and inflammatory cues. These encounters may also be facilitated by down-regulation of homeostatic chemokine receptors, such as CCR7, that usually maintain T cells in the T-zone areas. Expression of CCR7 in antigen-specific CD8 T cells declined at both mRNA and protein levels early after in vivo activation (Fig. S5). The extent of down-regulation was higher in KLRG1^{hi} cells compared with KLRG1^{lo} cells, however, and the latter regained partial surface expression of CCR7 by day 8 postinfection (Fig. S5*B*). These results are consistent with reported observations demonstrating that KLRG1^{lo} cells display a greater chemotactic response to the CCR7 ligand CCL19 and are localized within the T-zone areas of the spleen at day 8 postinfection (20). A previous study has shown that persistent Tg expression of CCR7 in P14 cells leads to sequestration of effector CD8 T cells within the splenic T zone (31). To determine whether this altered localization affects the differentiation of antigen-experienced CD8 T cells, we generated P14 TCR Tg mice that were also Tg for mouse CCR7 driven by a mouse CD4 promoter lacking the intronic transcriptional silencer, thus remaining active in both CD4 and CD8 T cells (32). In contrast to WT cells, CCR7 Tg P14 CD8 cells maintained cell surface expression of CCR7 after in vivo activation (Fig. 7*A*). Furthermore, fewer CCR7 Tg cells were found in blood compared with WT, indicating that altered CCR7 expression led to sequestration within lymphoid tissues (Fig. 7*B*). More strikingly, in both blood and spleen, a greater proportion of CCR7 Tg P14 cells were KLRG1^{lo} IL-7Rα^{hi} compared with WT cells (Fig. 7 *C* and *D*), suggesting that the former had less exposure to signals that drive terminal effector differentiation, such as antigen and inflammation. Indeed, at day 4 postinfection, we found WT P14 T cells localizing with viral antigen in the spleen, whereas CCR7 Tg P14 T cells were found mostly in the T-zone areas and away from viral antigen (Fig. 7*E*). These results suggest that in addition to the expression of inflammatory chemokine receptors, down-regulation of chemokine receptors that homeostatically position T cells within the T-zone areas of the spleen contributes to their exposure to antigen and inflammatory signals and has an impact on their fate determination.

Discussion

A number of studies have established that the magnitude and quality of CD8 T-cell effector and memory responses are influenced by T-cell precursor frequencies as well as by the extent and duration of antigen and inflammation (33–36). In this study, we demonstrated that chemokine receptors also affect CD8 T-cell differentiation in response to an infection and influence the quality and quantity of long-lived memory CD8 T cells. Absence of an inflammatory chemokine receptor, CXCR3, on CD8 T cells led to fewer short-lived effector cells and more memory precursor cells at the peak of the response. The long-lived memory CD8 T cells derived from this population had fewer cells with phenotypic characteristics of effector memory cells and displayed a more robust recall response than WT cells. Similarly, constitutive expression of a homeostatic chemokine receptor, CCR7, normally down-regulated on T-cell activation, led to development of more memory precursor cells. We found that in the absence of CXCR3, effector CD8 T cells were more localized in the T-cell zone than with viral antigen present in the marginal zone areas of the spleen. Similarly, persistent expression of CCR7, a homeostatic chemokine receptor that is usually down-regulated on T-cell activation, led to sequestration of effector CD8 T cells within the T-zone areas and away from antigen and skewed the CD8 T-cell

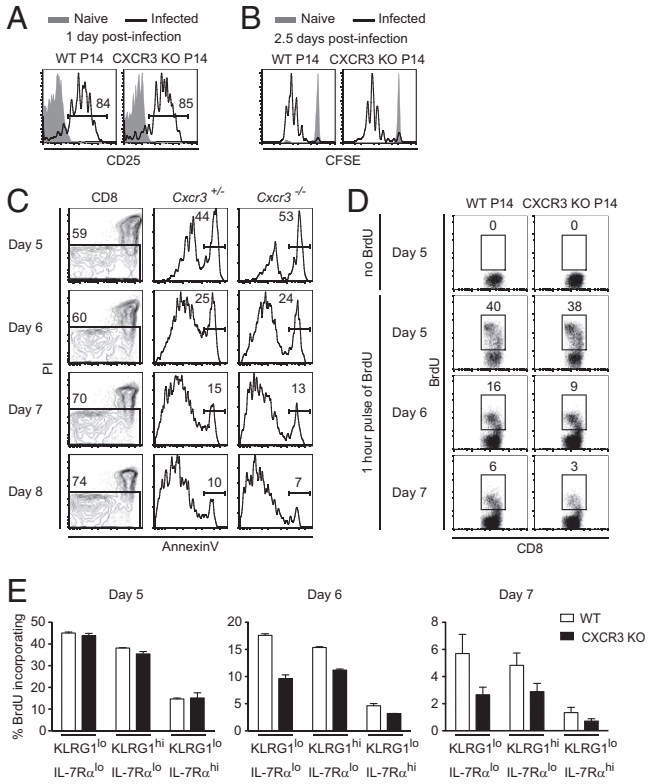

Fig. 6. CXCR3-deficient CD8 T cells show reduced proliferation during the later stages of infection. (*A*) Mice containing equal numbers of CD45.1/CD45.2 WT and CD45.1/CD45.1 CXCR3 KO P14 T cells were infected with LCMV. Histograms show CD25 expression on WT and CXCR3 KO P14 T cells in spleen at day 1 postinfection. (*B*) Equal numbers of CFSE-labeled CD45.1/CD45.2 WT and CD45.1/CD45.1 CXCR3 KO P14 T cells were transferred into C57BL/6 mice and then infected a day later with LCMV. Histograms show CFSE dilution of the indicated population within the spleen 2.5 d after infection. Data shown are representative of two independent experiments ($n = 4$). (*C*) C57BL/6 mice containing equal numbers of CD45.1/CD45.2 *Cxcr3*$^{+/-}$ and CD45.1/CD45.1 *Cxcr3*$^{-/-}$ P14 T cells were infected with LCMV, and the proportion of apoptotic cells in each population within the spleen was determined by flow cytometry at the indicated times. *Cxcr3*$^{+/-}$ and *Cxcr3*$^{-/-}$ P14 T cells were gated from CD8^{+} PI^{-} cells to determine the frequency of annexin V-positive apoptotic cells in each population. Data shown are representative of two mice at each time. (*D* and *E*) C57BL/6 mice containing equal numbers of CD45.1/CD45.2 WT and CD45.1/CD45.1 CXCR3 KO P14 T cells were infected with LCMV; at the indicated times after infection, they were pulsed with BrdU for 1 h and then analyzed by flow cytometry. (*D*) Dot plots show BrdU incorporation of WT and CXCR3 KO P14 T cells in spleen at the indicated times after infection. (*E*) Proportion of BrdU^{+} cells in KLRG1^{lo} IL-7R^{lo}, KLRG1^{hi} IL-7R^{lo}, and KLRG1^{lo} IL-7R^{hi} subsets of WT and CXCR3 KO P14 T-cell populations was determined by flow cytometry at the indicated times postinfection. Averages and SEM are shown. Data shown are representative of two independent experiments ($n = 4$ for each time).

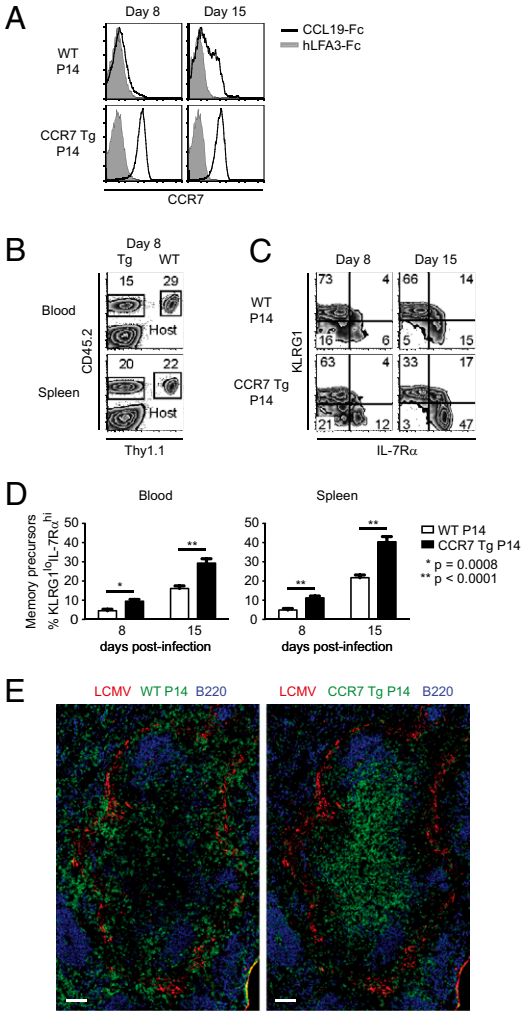

Fig. 7. Persistent CCR7 expression tips the balance toward development of more memory precursors than terminally differentiated effector CD8 T cells. (*A–D*) B6.BoyJ (CD45.1) mice containing equal numbers of Thy1.1^{+}, CD45.2^{+} WT and Thy1.2^{+}, CD45.2^{+} CCR7 Tg P14 T cells were infected with LCMV and analyzed at the indicated times. (*A*) Histograms show surface expression of CCR7 on WT and CCR7 Tg P14 T cells in spleen at the indicated times after infection. Gray histograms show the isotype control. (*B*) Frequencies of WT and CCR7 Tg P14 T cells in the blood and spleen were determined on day 8 postinfection. Plots are gated on CD8^{+} T cells. (*C*) Density plots show proportion of WT and CCR7 Tg CD8^{+} P14 T cells that express KLRG1 and IL-7Rα at the indicated times after infection. (*D*) Frequencies of KLRG1^{lo} IL-7Rα^{hi} memory precursor CD8 T cells within WT and CCR7 Tg P14 T-cell populations in blood and spleen were determined by flow cytometry at the indicated times after infection. Data shown are representative of three independent experiments ($n = 9$–11 mice per indicated time). The graphs show mean data ± SEM. Statistics were done using a two-tailed unpaired Student's *t* test. (*E*) C57BL/6 mice containing equal numbers of Thy1.1^{+}, CD45.2^{+} WT and Thy1.2^{+}, CD45.1^{+} CCR7 Tg P14 T cells were infected with LCMV. Sections were prepared from spleens at day 4 postinfection and stained for viral antigen, B220, and WT P14 (Thy1.1) and CCR7 Tg P14 (CD45.1) cells. (Scale bars: 100 μm.)

response toward more memory precursor cells. Because both of these changes in chemokine receptor expression affected localization of effector CD8 T cells, the observed effects on CD8 T-cell fate are most likely attributable to alterations in the access and exposure of these cells to antigen and inflammatory stimuli.

Differential localization of effector and memory CD8 T cells within secondary lymphoid tissues has been well described. A number of studies using various infection models and approaches have found effector CD8 T cells mostly localized in the red pulp of the spleen, with a small fraction residing in the T-cell zone at the peak of the response (7, 20, 37, 38). In contrast, memory CD8 T cells were found primarily in the T-cell areas of the spleen. A recent study showed that this differential localization of effector and memory CD8 T cells could be dictated by transcription factors that regulate CD8 T-cell fate. Localization of terminally differentiated KLRG1^{hi} IL-7Rα^{lo} effector CD8 T cells in the red pulp was dependent on expression of T-bet and Blimp-1 (20). In the absence of either of these transcription factors, CD8 T cells were located predominantly in the T-cell zone of the spleen and had phenotypic characteristics of long-lived memory CD8 T cells (KLRG1^{lo} IL-7Rα^{hi}). As part of regulating distinct transcriptional programming of terminal effector and memory

precursor CD8 T cells, T-bet and Blimp-1 may also regulate differential expression of various chemokine receptors, leading to altered localization of these cells within the spleen (20, 39). The molecular nature of the cues that guide effector CD8 T cells out of the T-cell zone is not well understood, however. Although CXCR3 is up-regulated on activated CD8 T cells, we found that up to day 5 postimmunization, it was not differentially expressed in terminal effector and memory precursor CD8 T cells. Furthermore, up to this time after infection, CXCR3 expression did not have an impact on the proportion of effector CD8 T cells that were KLRG1^{hi}, suggesting that this chemokine receptor is not a major determinant of CD8 T-cell fate. Absence of CXCR3 expression on CD8 effector T cells had three effects: (*i*) fewer cells became KLRG1^{hi} terminal effectors between days 5 and 8 postinfection, (*ii*) a smaller proportion of memory CD8 T cells had an effector memory phenotype, and (*iii*) both the quality and quantity of long-lived memory CD8 T cells were increased. Because the KLRG1^{hi} effector cells gradually down-regulated CXCR3 expression between days 5 and 8 postinfection through an unknown mechanism, it is most likely that these observed phenotypes are attributable to the presence of CXCR3 on the KLRG1^{lo} IL-7Rα^{lo} CD8 T-cell population. Several studies have shown that the majority of cells in this population are destined to become long-term memory cells of both central and effector phenotypes (3, 4). Consistent with the fate commitment with progressive differentiation model, however, these cells retain the potential to become terminally differentiated effector cells as well when given the appropriate signals (3). These results suggest that expression of CXCR3, particularly when the amount of antigen has diminished during the later stages of infection (between days 5 and 8), may facilitate encounter of the KLRG1^{lo} IL-7Rα^{lo} CD8 T cells with antigen and/or inflammatory signals that further drive their proliferation and differentiation into KLRG1^{hi} IL-7Rα^{lo} effector cells and away from becoming long-lived memory cells. Repeated exposure of memory precursor cells to antigen or inflammation is known to diminish the quality of the memory CD8 T cells that are generated (40). Therefore, it is likely that CXCR3 facilitates exposure of the KLRG1^{lo} IL-7Rα^{lo} CD8 T cells to antigen and inflammation, thus having a negative impact on the quality and phenotype of the memory CD8 T cells that are generated. Because IL-7 is mostly expressed in the T-zone areas of the spleen, it is also possible that the altered localization of CD8 T cells within these areas in the absence of CXCR3 or through constitutive expression of CCR7 may lead to better survival and eventual formation of long-lived memory cells. The fact that expression of IL-7R itself is not sufficient to drive differentiation of CD8 T cells toward memory argues against this possibility, however (41). Therefore, expression of an inflammatory chemokine receptor can tip the balance toward more terminal effector cells as well as having an impact on the quality of the memory CD8 T cells that are generated (Fig. S6).

Several recent studies on the role of the mTOR pathway in CD8 effector T cells have highlighted an important role for a metabolic switch in transitioning from memory precursor to mature long-lived CD8 T cells (25, 42, 43). Treatment of mice with rapamycin, an inhibitor of mTOR, during the course of infection with LCMV led to a phenotype very similar to that of CXCR3-deficient CD8 T cells: generation of fewer short-lived effector CD8 T cells and more memory precursor cells as well as an increase in both the quantity and quality of long-lived memory cells. In T cells, mTOR is activated by various cytokines as well as engagement of TCR by antigen, resulting in a switch from catabolic metabolism to anabolic metabolism (44, 45). Generation of long-lived memory T cells requires a reversal of this metabolic switch to the homeostatic catabolic state. Inhibition of mTOR presumably accelerates this return to the baseline metabolic state, resulting in a more robust, long-lived, memory T-cell population. Because CXCR3 deficiency phenocopies mTOR inhibition, it is possible that expression of CXCR3 leads to more encounters with antigen and inflammatory stimuli, resulting in further activation of mTOR in effector CD8 T cells. Further studies are necessary to determine if there were any links between expression of inflammatory chemokine receptors and the metabolic state of effector CD8 T cells.

Several proinflammatory cytokines have been shown to act as "signal 3" and affect CD8 T-cell responses to various infections (46). In particular, absence of IFN-γ leads to a reduction in expansion of CD8 T cells in response to an LCMV infection (47). Most of this effect is attributable to direct action of IFN-γ on CD8 T cells (48). Nevertheless, because IFN-γ is an inducer of CXCR3 ligands, in light of our findings, some of the effects of this cytokine could be mediated indirectly through recruitment of effector CD8 T cells to antigen, leading to further expansion or decreased potential to form memory T cells. Furthermore, because production of CXCR3 ligands is most likely secondary to local production of IFN-γ by other activated T cells, recruitment of CXCR3-expressing effector CD8 T cells to these sites will also expose them directly to more IFN-γ. Thus, the IFN-γ and CXCR3 ligands together may provide a positive feedback loop for further exposure of effector CD8 T cells to antigen and inflammation. Although we focused on localization of T cells within the spleen in this study, it is also possible that in other infected tissues, IFN-γ and CXCR3 may play a similar role in exposure of effector CD8 T cells to antigen and proinflammatory cytokines.

Our study did not find a major role for CXCR3 in early recruitment, activation, and expansion of CD8 T cells, which is consistent with lack of expression of this receptor on the majority of naive CD8 T cells. CXCR3 expression on a minor population of naive P14 cells gave these cells a slight proliferative advantage, however. In addition, retroviral-mediated forced expression of CXCR3 at an early time in T-cell activation led to an increase in the magnitude of the CD8 T-cell response. Because CXCR3 is constitutively expressed at high levels on memory CD8 T cells and its ligands are also expressed shortly after infection, we expected that WT memory CD8 T cells would have an advantage over CXCR3-deficient memory cells in a secondary recall response. Surprisingly, we found that CXCR3 KO memory CD8 T cells had a larger secondary response than WT cells, suggesting that absence of CXCR3 led to development of qualitatively superior memory CD8 T cells (Fig. S6). In addition, these results indicate that CXCR3 is not necessary for a recall response to LCMV infection. This could be attributable to redundancy in expression of inflammatory chemokine receptors, such as CXCR6, which may facilitate encounter of memory CD8 T cells with antigen-presenting cells. These results also do not completely rule out a role for CXCR3 in a secondary response, because whatever competitive advantage expression of CXCR3 might have offered was overshadowed by qualitative differences between WT and CXCR3 KO memory CD8 T cells.

During the acute phase of infection, although CXCR3-deficient effector cells did not localize to antigen in the marginal zone areas of the spleen, they were readily found in blood and other tissues, indicating that this receptor was not necessary for either egress from lymphoid tissues or recruitment to other sites of infection. One study has implicated a role for another inflammatory chemokine receptor, CCR5, in guiding CD8 effector T cells to sites of antigen-specific dendritic cell–CD4 T-cell interactions to receive necessary help to form a functional memory population (49). Because CXCR3-deficient memory CD8 T cells demonstrated a robust response to a secondary challenge, expression of this receptor on CD8 effector T cells is not necessary to receive CD4 T-cell help. These results suggest that each inflammatory chemokine receptor may play a unique role in the development and function of CD8 T cells. Further investigation is necessary to address whether these differences can be generalized to other infections or immunization protocols and to determine the role of

other inflammatory chemokine receptors, such as CXCR6, that are up-regulated on activated CD8 T cells (50).

In this study, we showed that alterations in chemokine receptor expression can alter distribution of effector CD8 T cells within lymphoid tissues and have an impact on their differentiation and generation of memory CD8 T cells. Further studies on the role of various chemokine receptors and other guidance cues will advance our understanding of the interplay between these signals, localization within tissue microenvironments, and shaping of the effector and memory T-cell responses. In addition, it will be interesting to determine the role of chemokine receptors in repeated exposure of CD8 T cells to antigen in a chronic viral infection and their impact on T-cell exhaustion. Our findings suggest that targeting chemokine receptors, such as CXCR3, as part of vaccination protocols for protection against infections or cancer, may provide an approach to generate a more robust memory CD8 T-cell response.

Materials and Methods

Mice. C57BL/6 (CD45.2), B6.BoyJ (CD45.1), and Thy1.1 mice were purchased from the Jackson Laboratory or the National Cancer Institute. CD45.1/CD45.2 P14 and Thy1.1 P14 mice bearing the D^bGP33-specific TCR were maintained in our animal colony. *Cxcr3*$^{-/-}$ mice were a generous gift from C. Gerard (Children's Hospital, Harvard Medical School, Boston, MA). CCR7 Tg mice were a generous gift from N. Killeen (University of California, San Francisco, CA). All animals were housed in the specific pathogen-free facility at the University of California, San Francisco, and were treated according to protocols approved by university animal care ethics and veterinary committees in accordance with guidelines of the US National Institutes of Health.

Infection, Adoptive Transfer, and Bone Marrow Chimeras. LCMV Armstrong was propagated on BHK cells and titered on Veros cells as described (27). Unless indicated below, P14 chimeric mice were generated by adoptive transfer of 2×10^4 WT and 2×10^4 CXCR3 KO or 2×10^4 WT and 2×10^4 CCR7 Tg P14 T cells into C57BL/6 recipients that were infected i.p. 1–3 d later with 2×10^5 PFU LCMV Armstrong. A total of 2×10^5 P14 T cells were adoptively transferred for the sorting of KLRG^{hi} and KLRG1^{lo} cells and for the retroviral transductions; 2×10^5 to 1×10^6 P14 T cells were adoptively transferred for localization experiments; and 1×10^6 P14 cells were transferred for CFSE dilution assays. Mice were infected i.v. with 2×10^6 PFU LCMV for secondary infections, and they were infected i.p. with 2×10^6 PFU LCMV for immunofluorescence. To generate mixed bone marrow chimeras, 6- to 8-wk-old C57BL/6 mice were lethally irradiated by γ-irradiation from a Cesium source. Bone marrow cells from WT and *Cxcr3*$^{-/-}$ mice were mixed in a 1:1 ratio and used to reconstitute the irradiated mice. The mice were maintained on antibiotics for 6 wk during reconstitution and then bled to determine the proportion of CD8 T cells derived from each donor. Mice were infected i.p. with 2×10^5 PFU LCMV Armstrong, and LCMV-specific CD8 T cells were analyzed after infection.

Isolation of Lymphocytes from Nonlymphoid Organs. Mice were perfused with PBS before removal, mincing, and passage of liver and lung through a 70-μm filter mesh. Lymphocytes were enriched from the homogenates at the interface of a 40–60% discontinuous Percoll (GE Healthcare Bio-Sciences AB) gradient.

Cell Sorting. 8w?>Marginal zone macrophages and marginal metallophilic macrophages were sorted from uninfected and LCMV-infected spleens at day 1 postinfection. Macrophages were enriched by negative selection using a biotinylated antibody mixture (CD4, CD19, and Thy1.2), streptavidin microbeads, and an autoMACS instrument (Miltenyi Biotec). Enriched cells were sorted using antibodies to CD11b, CD169, CD209b, and DAPI on a FACSAria (BD Biosciences). For some experiments, naive, effector, or memory P14 T cells were enriched by negative selection using a biotinylated antibody mixture (CD4, CD19, and I-A^b), streptavidin microbeads, and an autoMACS instrument. Enriched cells were stained with antibodies to CD8 and CXCR3 to sort for naive cells; antibodies to CD8, CD45.1, and KLRG1 to sort for effector cells; or antibodies to CD8, CD45.1, CD90.1, and CD62L to sort for memory cells. The purity of FACS-sorted T cells was ~99%, and the purity of enriched T cells isolated by AutoMACS was ~90%.

Antibodies and Reagents. Anti-LCMV serum and MHC I tetramers were generous gifts from R. Ahmed (Emory University School of Medicine, Atlanta, GA). CCL19-Fc was a generous gift from J. Cyster (University of California, San Francisco, CA). All antibodies were purchased from Biolegend except for anti-mouse KLRG1 (Southern Biotech and eBioscience); anti-mouse CXCL9 (R&D Systems); anti-mouse CD25, CD45.1, CD62L, CD90.1, CD90.2, CD169, and CD209b (eBioscience); anti-mouse CD45R and CD122 (BD Pharmingen); anti-mouse CD4, CD11b, CD16/32, CD19, and Ly6G (University of California, San Francisco Antibody Core Facility); anti-human Granzyme B (Invitrogen); anti-human LFA3 (Biogen); and anti-human IgG, anti-guinea pig IgG, and anti-goat IgG (Jackson Immunoresearch).

Quantitative RT-PCR. Previously snap-frozen tissues were homogenized, and RNA was isolated using TRIzol Reagent (Invitrogen) according to the manufacturer's instructions. Total RNA was reverse-transcribed using an M-MLV reverse transcriptase kit (Invitrogen). The resulting cDNA was analyzed for expression of different genes by quantitative PCR using FastStart Universal SYBR Green Master (ROX; Roche) or AmpliTaq Gold DNA polymerase (Applied Biosystems) on an ABI 7300 Real Time PCR System (Applied Biosystems). Relative gene expression was normalized to the housekeeping genes, hypoxanthine phosphoribosyltransferase (*Hprt*) or glyceraldehyde 3-phosphate dehydrogenase (*Gapdh*). PCR primer pairs were as follows: *Hprt*: 5′-AGGTTGCAAGCTTGCTGGT and 5′-TGAAGTACTCATTATAGTCAAGGGCA, probe 5′-TGTTGGATACAGGCCAGACTTTGTTGGAT; *Gapdh*: 5′-GGTCTACATGTTCCAGTATGACTCCAC and 5′-GGGTCTCGCTCCTGGAAGAT; *Cxcl9*: 5′-CCCAAGCCCCAATTGCA and 5′-ATTTGCCGAGTCCGGATCTAG, probe 5′-CAAAACTGAAATCATTGCTACACTGAAGAACGGAG; *Cxcl10*: 5′-AGCACCATGAACCCAA and 5′-CAGTTGCAGCGGACCGTC, probe 5′-TGGGACTCAAGGGATCCCTCTCGC; and LCMV *S segment*: 5′-CGTCATTGAGCGGAGTCTGT and 5′-AGATCATGAGGTCTGAAAGGC.

Retroviral Transduction. The MSCV-IRES-Thy1.1 vector was a generous gift from A. Abbas (University of California, San Francisco, CA). cDNA was made from LCMV-infected spleens, and *Cxcr3* was amplified by PCR using the following primers: 5′-TAGTAGGCGGCCGCACCATGTACCTTGAGGTTAGTGAACGTCAA and 5′-TAGTAGATCGATGAATTACAAGCCCAGGTAGGAGGC. The amplified product was cloned into NotI and ClaI restriction sites of the MSCV-IRES-Thy1.1 vector, and the sequence was verified by automated sequencing. Retroviruses were packaged by transient transfection of Phoenix cells using Lipofectamine 2000 (Invitrogen) according to the manufacturer's instructions. For retroviral transduction of P14 T cells, CD45.1 CXCR3 KO P14 mice were infected i.v. with 2×10^6 PFU LCMV Armstrong. One day later, P14 T cells from infected spleens were transduced with empty MSCV-IRES-Thy1.1 vector or MSCV-CXCR3-IRES-Thy1.1 vector by spin infection ($850 \times g$ for 2 h at 30 °C). C57BL/6 recipients were infected i.p. with 2×10^5 PFU LCMV Armstrong 1 to 2 h before receiving 2×10^5 transduced CXCR3 KO P14 T cells.

CFSE, BrdU, Annexin V, Chemokine Receptors, and Chemotaxis. Spleens and lymph nodes were enriched for naive P14 T cells as described above. Enriched P14 T cells were incubated in PBS with 7 μM CFSE (Invitrogen) for 20 min at room temperature. The cells were quenched with FBS and washed in RPMI. A total of 1×10^6 CFSE-labeled P14 T cells were adoptively transferred into naive C57BL/6 mice. The next day, recipients were infected i.v. with 2×10^5 PFU LCMV Armstrong. Mice were injected i.p. with 1 mg BrdU (BD Pharmingen) at 5, 6, and 7 d postinfection. Spleens were harvested 1 h later, and an FITC BrdU Flow Kit (BD Pharmingen) was used according to the manufacturer's instructions. An Annexin V-FITC Apoptosis Detection Kit I (BD Pharmingen) was used according to the manufacturer's instructions. To stain for chemokine receptors, cells were first incubated for 30 min at 37 °C. For CCR7, cells were stained with CCL19-Fc or hLFA3-Fc as a control for 30 min. Chemotaxis assays were performed as described (50).

Intracellular Staining. Spleen cells were cultured in media as described in the presence of 1 μg/mL GolgiPlug (BD Biosciences) and 0.2 μg/mL LCMV GP33-41 peptide (27). After 5 h of culture, cells were stained for surface markers, washed, fixed with formaldehyde, and then stained for intracellular cytokines in the presence of 0.5% saponin.

Immunofluorescence and Imaging. Mice were killed, and spleens were embedded in optimum cutting temperature embedding compound (Sakura Finetek) and then frozen. Sections (6 μm thick) were cut with a cryomicrotome (Leica Microsystems) and collected onto Superfrost/Plus microscope slides (Fisher Scientific). Acetone-fixed sections were blocked with nonfat dry milk and stained with fluorescent antibodies for 45 min in Tris-buffered saline containing 0.1% BSA, 1% normal mouse serum, and 1% normal donkey serum. Spleen sections were imaged using a Zeiss Axio Imager M1 upright microscope (Carl Zeiss Microimaging, Inc.), a Zeiss objective with a magnification

of 20× and N.A. of 0.8, and an AxioCam MRc camera. The Axiovision software program MosaiX was used to generate a stitched image from individual tiles.

Statistical Analysis. Prism software (GraphPad Software, Inc.) was used for all statistical analyses. All results are expressed as mean ± SEM. Two groups were compared using the two-tailed Student's *t* test or two-way ANOVA as noted in figure legends. $P < 0.05$ was considered significant.

ACKNOWLEDGMENTS. We are grateful for the generosity of the following people: Craig Gerard for the CXCR3 KO mice; Jason Cyster for the CCL19-Fc fusion protein and use of equipment; Hong Wu and Rafi Ahmed for tetramers and helpful discussions, respectively; Art Weiss and Richard Locksley for use of various equipment; Chris Allen for use of his microscope; and Shomyseh Sanjabi for critically reading the manuscript. We appreciate help with cell sorting from Cliff McArthur, Zhi-en Wang, and Stephen Chmura. J.K.H. was supported, in part, by an Endocrinology Training Grant from the National Institutes of Health (Grant 5T32-DK07418). J.M.C. was supported by a Graduate Research Fellowship from the National Science Foundation. M.M. was supported, in part, by the Rosalind Russell Medical Research Center for Arthritis and National Institutes of Health Grant 1R01AI074694.

1. Williams MA, Bevan MJ (2007) Effector and memory CTL differentiation. *Annu Rev Immunol* 25:171–192.
2. Gerlach C, et al. (2010) One naive T cell, multiple fates in CD8+ T cell differentiation. *J Exp Med* 207:1235–1246.
3. Joshi NS, et al. (2007) Inflammation directs memory precursor and short-lived effector CD8(+) T cell fates via the graded expression of T-bet transcription factor. *Immunity* 27:281–295.
4. Sarkar S, et al. (2008) Functional and genomic profiling of effector CD8 T cell subsets with distinct memory fates. *J Exp Med* 205:625–640.
5. Bromley SK, Peterson DA, Gunn MD, Dustin ML (2000) Cutting edge: Hierarchy of chemokine receptor and TCR signals regulating T cell migration and proliferation. *J Immunol* 165:15–19.
6. Matloubian M, et al. (2004) Lymphocyte egress from thymus and peripheral lymphoid organs is dependent on S1P receptor 1. *Nature* 427:355–360.
7. Potsch C, Vöhringer D, Pircher H (1999) Distinct migration patterns of naive and effector CD8 T cells in the spleen: Correlation with CCR7 receptor expression and chemokine reactivity. *Eur J Immunol* 29:3562–3570.
8. Sallusto F, et al. (1999) Switch in chemokine receptor expression upon TCR stimulation reveals novel homing potential for recently activated T cells. *Eur J Immunol* 29: 2037–2045.
9. Sallusto F, Lenig D, Mackay CR, Lanzavecchia A (1998) Flexible programs of chemokine receptor expression on human polarized T helper 1 and 2 lymphocytes. *J Exp Med* 187:875–883.
10. Campanella GS, et al. (2008) Chemokine receptor CXCR3 and its ligands CXCL9 and CXCL10 are required for the development of murine cerebral malaria. *Proc Natl Acad Sci USA* 105:4814–4819.
11. Hancock WW, et al. (2000) Requirement of the chemokine receptor CXCR3 for acute allograft rejection. *J Exp Med* 192:1515–1520.
12. Nakanishi Y, Lu B, Gerard C, Iwasaki A (2009) CD8(+) T lymphocyte mobilization to virus-infected tissue requires CD4(+) T-cell help. *Nature* 462:510–513.
13. Thapa M, Carr DJ (2009) CXCR3 deficiency increases susceptibility to genital herpes simplex virus type 2 infection: Uncoupling of CD8+ T-cell effector function but not migration. *J Virol* 83:9486–9501.
14. Wuest TR, Carr DJ (2008) Dysregulation of CXCR3 signaling due to CXCL10 deficiency impairs the antiviral response to herpes simplex virus 1 infection. *J Immunol* 181: 7985–7993.
15. Zhang B, Chan YK, Lu B, Diamond MS, Klein RS (2008) CXCR3 mediates region-specific antiviral T cell trafficking within the central nervous system during West Nile virus encephalitis. *J Immunol* 180:2641–2649.
16. Farber JM (1990) A macrophage mRNA selectively induced by gamma-interferon encodes a member of the platelet factor 4 family of cytokines. *Proc Natl Acad Sci USA* 87:5238–5242.
17. Luster AD, Ravetch JV (1987) Genomic characterization of a gamma-interferon-inducible gene (IP-10) and identification of an interferon-inducible hypersensitive site. *Mol Cell Biol* 7:3723–3731.
18. Ohmori Y, Hamilton TA (1990) A macrophage LPS-inducible early gene encodes the murine homologue of IP-10. *Biochem Biophys Res Commun* 168:1261–1267.
19. Vanguri P, Farber JM (1990) Identification of CRG-2. An interferon-inducible mRNA predicted to encode a murine monokine. *J Biol Chem* 265:15049–15057.
20. Jung YW, Rutishauser RL, Joshi NS, Haberman AM, Kaech SM (2010) Differential localization of effector and memory CD8 T cell subsets in lymphoid organs during acute viral infection. *J Immunol* 185:5315–5325.
21. Christensen JE, de Lemos C, Moos T, Christensen JP, Thomsen AR (2006) CXCL10 is the key ligand for CXCR3 on CD8+ effector T cells involved in immune surveillance of the lymphocytic choriomeningitis virus-infected central nervous system. *J Immunol* 176: 4235–4243.
22. Hsieh MF, et al. (2006) Both CXCR3 and CXCL10/IFN-inducible protein 10 are required for resistance to primary infection by dengue virus. *J Immunol* 177:1855–1863.
23. Kohlmeier JE, et al. (2009) CXCR3 directs antigen-specific effector CD4+ T cell migration to the lung during parainfluenza virus infection. *J Immunol* 183:4378–4384.
24. Stiles LN, Liu MT, Kane JA, Lane TE (2009) CXCL10 and trafficking of virus-specific T cells during coronavirus-induced demyelination. *Autoimmunity* 42:484–491.
25. Araki K, et al. (2009) mTOR regulates memory CD8 T-cell differentiation. *Nature* 460: 108–112.
26. Sallusto F, Lenig D, Förster R, Lipp M, Lanzavecchia A (1999) Two subsets of memory T lymphocytes with distinct homing potentials and effector functions. *Nature* 401: 708–712.
27. Wherry EJ, et al. (2003) Lineage relationship and protective immunity of memory CD8 T cell subsets. *Nat Immunol* 4:225–234.
28. Seiler P, et al. (1997) Crucial role of marginal zone macrophages and marginal zone metallophils in the clearance of lymphocytic choriomeningitis virus infection. *Eur J Immunol* 27:2626–2633.
29. Ahmed R, Gray D (1996) Immunological memory and protective immunity: Understanding their relation. *Science* 272:54–60.
30. Kaech SM, Wherry EJ (2007) Heterogeneity and cell-fate decisions in effector and memory CD8+ T cell differentiation during viral infection. *Immunity* 27:393–405.
31. Unsoeld H, Voehringer D, Krautwald S, Pircher H (2004) Constitutive expression of CCR7 directs effector CD8 T cells into the splenic white pulp and impairs functional activity. *J Immunol* 173:3013–3019.
32. Kwan J, Killeen N (2004) CCR7 directs the migration of thymocytes into the thymic medulla. *J Immunol* 172:3999–4007.
33. Badovinac VP, Porter BB, Harty JT (2002) Programmed contraction of CD8(+) T cells after infection. *Nat Immunol* 3:619–626.
34. Kaech SM, Ahmed R (2001) Memory CD8+ T cell differentiation: initial antigen encounter triggers a developmental program in naïve cells. *Nat Immunol* 2:415–422.
35. Mercado R, et al. (2000) Early programming of T cell populations responding to bacterial infection. *J Immunol* 165:6833–6839.
36. Zehn D, Lee SY, Bevan MJ (2009) Complete but curtailed T-cell response to very low-affinity antigen. *Nature* 458:211–214.
37. Dauner JG, Williams IR, Jacob J (2008) Differential microenvironment localization of effector and memory CD8 T cells. *J Immunol* 180:291–299.
38. Khanna KM, McNamara JT, Lefrançois L (2007) In situ imaging of the endogenous CD8 T cell response to infection. *Science* 318:116–120.
39. Rutishauser RL, et al. (2009) Transcriptional repressor Blimp-1 promotes CD8(+) T cell terminal differentiation and represses the acquisition of central memory T cell properties. *Immunity* 31:296–308.
40. Wherry EJ, McElhaugh MJ, Eisenlohr LC (2002) Generation of CD8(+) T cell memory in response to low, high, and excessive levels of epitope. *J Immunol* 168:4455–4461.
41. Hand TW, Morre M, Kaech SM (2007) Expression of IL-7 receptor alpha is necessary but not sufficient for the formation of memory CD8 T cells during viral infection. *Proc Natl Acad Sci USA* 104:11730–11735.
42. Pearce EL, et al. (2009) Enhancing CD8 T-cell memory by modulating fatty acid metabolism. *Nature* 460:103–107.
43. Prlic M, Bevan MJ (2009) Immunology: A metabolic switch to memory. *Nature* 460: 41–42.
44. Jones RG, Thompson CB (2007) Revving the engine: Signal transduction fuels T cell activation. *Immunity* 27:173–178.
45. Sinclair LV, et al. (2008) Phosphatidylinositol-3-OH kinase and nutrient-sensing mTOR pathways control T lymphocyte trafficking. *Nat Immunol* 9:513–521.
46. Haring JS, Badovinac VP, Harty JT (2006) Inflaming the CD8+ T cell response. *Immunity* 25:19–29.
47. Badovinac VP, Tvinnereim AR, Harty JT (2000) Regulation of antigen-specific CD8+ T cell homeostasis by perforin and interferon-gamma. *Science* 290:1354–1358.
48. Whitmire JK, Tan JT, Whitton JL (2005) Interferon-gamma acts directly on CD8+ T cells to increase their abundance during virus infection. *J Exp Med* 201:1053–1059.
49. Castellino F, et al. (2006) Chemokines enhance immunity by guiding naive CD8+ T cells to sites of CD4+ T cell-dendritic cell interaction. *Nature* 440:890–895.
50. Matloubian M, David A, Engel S, Ryan JE, Cyster JG (2000) A transmembrane CXC chemokine is a ligand for HIV-coreceptor Bonzo. *Nat Immunol* 1:298–304.